REGULAR ARTICLE

Polymer Journal

Change in Characteristics of Wormlike Micelles of Hexaoxyethylene Tetradecyl and Decyl Ethers ($C_{14}E_6$ and $C_{10}E_6$) with Uptake of *n*-Dodecane

*By Marina OCHI, Sayaka MATSUE, and Yoshiyuki EINAGA**

Wormlike micelles of the surfactant hexaoxyethylene tetradecyl and decyl ethers $C_{14}E_6$ and $C_{10}E_6$ were characterized by static (SLS) and dynamic light scattering (DLS) experiments to examine effects of uptake of *n*-dodecane on the micellar characteristics. The SLS results have been successfully analyzed by the light scattering theory for micelle solutions to yield the molar mass $M_w(c)$ as a function of concentration c along with the cross-sectional diameter d of the micelle. The apparent hydrodynamic radius $R_{H,app}(c)$ determined by DLS as a function of c has also been successfully analyzed by the fuzzy cylinder theory which takes into account the hydrodynamic and direct collision interactions among micelles, providing us with the values of the stiffness parameter λ^{-1}. It has been found that although the micellar length L_w increases with increasing surfactant mass concentration c and the d and λ^{-1} values increase with increasing *n*-dodecane content w_d, as in the case of various C_iE_j micelles containing *n*-alcohol, the values of M_w, L_w, and $R_{H,app}$ for all the micelles examined decrease or hardly vary with increasing w_d contrary to the micelles containing *n*-alcohol. This finding may reflect the fact that the addition of *n*-dodecane into the micelles weakens hydrophilic interactions among polyoxyethylene chains of the surfactant molecules and water, making the micelles unstable, and then leading to collapse them into micelles of the smaller size.

KEY WORDS: Wormlike Micelle / Light Scattering / Cloud Point Curve / Diffusion Coefficient / Hydrodynamic Radius / Polyoxyethylene Alkyl Ether / Surfactant /

In this series of work on micelle solutions of nonionic surfactant polyoxyethylene alkyl ethers $H(CH_2)_i(OCH_2CH_2)_j$-OH (abbreviated C_iE_j), we have characterized the wormlike C_iE_j micelles with various i and j containing *n*-alcohols, *n*-dodecanol or *n*-octanol,[1–5] and *n*-dodecane[6] by static (SLS) and dynamic light scattering (DLS) measurements in order to explore effects of uptake of *n*-alcohol or *n*-dodecane into the micelles on the micellar characteristics. It has been demonstrated that the SLS results (the excess Rayleigh ratio) as a function of surfactant concentration c are successfully analyzed by a molecular thermodynamic theory[7,8] formulated with the wormlike spherocylinder model to provide us with molar mass $M_w(c)$ of the micelle at a specified c along with the cross-sectional diameter d of the spherocylinder, as in the case of the micelle solutions of pure C_iE_j and binary C_iE_j mixtures.[9–16] The DLS results have been also successfully analyzed in a similar fashion to the micelle solutions of pure C_iE_j and their binary mixtures with the aid of the fuzzy cylinder theory,[17–20] thereby yielding the concentration-dependent micellar growth by separating contributions of the enhancement of hydrodynamic interactions among micelles with increasing concentration to the apparent hydrodynamic radius $R_{H,app}$, which is directly obtained from DLS experiment. The analyses have yielded the values of the stiffness parameter λ^{-1} and shown that the molar mass M_w dependence of the hydrodynamic radius R_H is quantitatively represented by the hydrodynamic theory based on the wormlike spherocylinder models.[21–23]

It has been found for the micelles of $C_{12}E_6$, $C_{10}E_5$, $C_{12}E_5$, $C_{10}E_6$, and $C_{14}E_6$ that the values of the micellar length L, d, and λ^{-1} become larger as the *n*-dodecanol or *n*-octanol content in the micelles increases.[1–5] On the other hand, the values of M_w, L_w, and $R_{H,app}$ for the micelles of $C_{12}E_5$, $C_{12}E_6$, and $C_{12}E_7$ containing *n*-dodecane decrease with increasing *n*-dodecane content contrary to the micelles containing *n*-alcohol,[6] although the micellar length L_w increases with increasing surfactant mass concentration c and the values of d and λ^{-1} increase with increasing *n*-dodecane content w_d, as in the case of the micelles containing *n*-alcohol. This finding may be attributed to the fact that the addition of *n*-dodecane into the micelles weakens hydrophilic interactions among polyoxyethylene chains of the surfactant molecules and water, making the micelles unstable, and then leading to collapse them into micelles of the smaller size.

In this work, we have studied on the micelles in the $C_{14}E_6$ + *n*-dodecane + water and $C_{10}E_6$ + *n*-dodecane + water systems by SLS and DLS measurements in order to investigate effects of uptake of *n*-alcane on the variation of the micellar characteristics such as the micellar length, cross-sectional diameter, and stiffness in comparison with the case of uptake of *n*-alcohol. In particular, variation of the effects with the alkyl chain length i of the surfactants C_iE_6 (i = 10, 12, and 14) is examined, while in the previous work,[6] variation with the oxyethylene chain length j of the surfactants $C_{12}E_j$ (j = 5, 6, and 7) has been investigated. To this end, our previous results[1,6] for the $C_{12}E_6$ + *n*-dodecane micelles are reproduced in this paper for comparison. We follow the technique

Department of Chemistry, Nara Women's University, Nara 630-8506, Japan
*To whom correspondence should be addressed (E-mail: einaga@cc.nara-wu.ac.jp).

 doi:10.1295/polymj.PJ2007246

mentioned above to characterize "isolated" micelles at finite c by separate evaluation of the thermodynamic and hydrodynamic interactions among micelles.

EXPERIMENTAL

Materials

The surfactant $C_{14}E_6$ and $C_{10}E_6$ samples and *n*-dodecane were purchased from Nikko Chemicals Co. Ltd. and Nakarai-tesque Co., respectively, and used without further purification. The solvent water used was high purity (ultrapure) water prepared with Simpli Lab water purification system of Millipore Co.

Cloud Point

Cloud-point temperature of a given micelle solution was determined as the temperature at which the intensity of the laser light transmitted through the solution abruptly decreased when temperature was gradually raised.

$C_{14}E_6$ and $C_{10}E_6$ micelle solutions were prepared by dissolving $C_{14}E_6$ or $C_{10}E_6$ in water with adding appropriate amount of *n*-dodecane with a microliter syringe (Hamilton). Complete mixing and micelle formation were achieved by stirring the solutions using a magnetic stirrer for at least 1 d. The weight fractions w of micelle solutions were determined gravimetrically and converted to mass concentrations c by the densities ρ of the solutions given below. Throughout this paper, w and c denote the weight fraction and mass concentration of ($C_{14}E_6$ or $C_{10}E_6$) + *n*-dodecane in the ($C_{14}E_6$ or $C_{10}E_6$) + water + *n*-dodecane ternary solutions. *n*-Dodecane content in the ($C_{14}E_6$ or $C_{10}E_6$) + *n*-dodecane mixture is represented by its weight fraction w_d.

Static Light Scattering

The scattering intensities were measured for micelle solutions of $C_{14}E_6$ + *n*-dodecane with various w_d at 25.0 °C and for those $C_{10}E_6$ + *n*-dodecane with various w_d at 40.0 °C. The ratio $Kc/\Delta R_\theta$ was obtained for each solution as a function of the scattering angle θ ranging from 30 to 150° and extrapolated to zero scattering angle to evaluate $Kc/\Delta R_0$. Here, c is the mass concentration of the surfactant + *n*-dodecane, ΔR_θ is the excess Rayleigh ratio, and K is the optical constant. The plot of $Kc/\Delta R_\theta$ *vs.* $\sin^2(\theta/2)$ affords a good straight line for all the micelle solutions studied.

The apparatus used is an ALV DLS/SLS-5000/E light scattering photogoniometer and correlator system with vertically polarized incident light of 632.8 nm wavelength from a Uniphase Model 1145P He-Ne gas laser.

The micellar solutions were prepared in the same way as those for the cloud-point measurements described above. The experimental procedure is the same as described before.[2,9–16] In the present study, we have treated the micelle solutions as the binary system which consists of micelles containing *n*-dodecane as a solute and water as a solvent.

The results for the refractive index increment $(\partial n/\partial c)_{T,p}$ measured at 632.8 nm with a Union Giken R601 differential refractometer are summarized as (in cm^3/g), where T is the absolute temperature and p is the pressure:

For $C_{14}E_6$ + *n*-dodecane + water at 20.0 °C ≤ T ≤ 30.0 °C,

$$(\partial n/\partial c)_{T,p} = 0.142 - 3.20 \times 10^{-4}(T - 273.15) \quad (w_d = 0.0293) \tag{1}$$

$$(\partial n/\partial c)_{T,p} = 0.143 - 3.20 \times 10^{-4}(T - 273.15) \quad (w_d = 0.0509) \tag{2}$$

$$(\partial n/\partial c)_{T,p} = 0.141 - 3.20 \times 10^{-4}(T - 273.15) \quad (w_d = 0.1008) \tag{3}$$

For $C_{10}E_6$ + *n*-dodecane + water at 30.0 °C ≤ T ≤ 40.0 °C,

$$(\partial n/\partial c)_{T,p} = 0.1333 - 1.82 \times 10^{-4}(T - 273.15) \quad (w_d = 0.0250) \tag{4}$$

$$(\partial n/\partial c)_{T,p} = 0.1327 - 2.10 \times 10^{-4}(T - 273.15) \quad (w_d = 0.0501) \tag{5}$$

$$(\partial n/\partial c)_{T,p} = 0.1326 - 2.58 \times 10^{-4}(T - 273.15) \quad (w_d = 0.1003) \tag{6}$$

It is to be noted that the possible effects that the solvent water may include negligible amount of *n*-dodecane were not taken into consideration and that $(\partial n/\partial c)_{T,p}$ was measured with reference to pure water. The effects were also safely neglected in the light scattering measurements.

Dynamic Light Scattering

DLS measurements were carried out to determine the translational diffusion coefficient D and then the apparent hydrodynamic radius $R_{H,app}$ for the micelles by the use of the same apparatus and light source as used in the SLS studies described above. All the test solutions studied are the same as those used in the SLS studies. From the D values obtained by the cumulant method for the normalized autocorrelation function $g^{(2)}(t)$, $R_{H,app}$ has been evaluated by the defining equation[2,24–26]

$$D = \frac{(1 - vc)^2 M_w k_B T}{6\pi\eta_0 R_{H,app}} \left(\frac{Kc}{\Delta R_0}\right) \tag{7}$$

where v is the partial specific volume of the solute (micelle), k_B is the Boltzmann constant, and η_0 is the solvent viscosity.

Density

For all the micelle solutions containing *n*-dodecane, the solution density ρ has been found to be independent of micelle weight fraction w and *n*-dodecane content w_d at every temperature examined, *i.e.*, from 20.0 to 30.0 °C for $C_{14}E_6$ micelle solutions and from 30.0 to 40.0 °C for $C_{10}E_6$ micelle

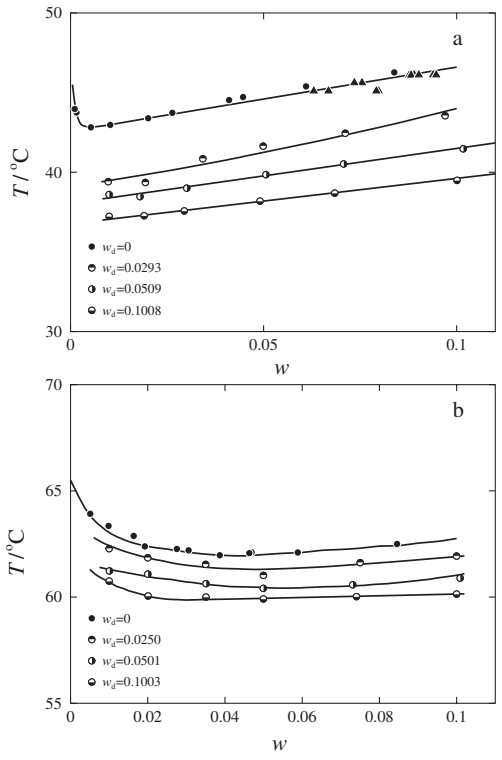

Figure 1. Cloud point curves for the $C_{14}E_6$ + *n*-dodecane + water system (a) and for the $C_{10}E_6$ + *n*-dodecane + water system (b): w_d, weight fraction of *n*-dodecane in the ($C_{14}E_6$ or $C_{10}E_6$) + *n*-dodecane mixture; triangles in (a) represent the binodal points. The data points for $w_d = 0$ are the literature results.[9,11]

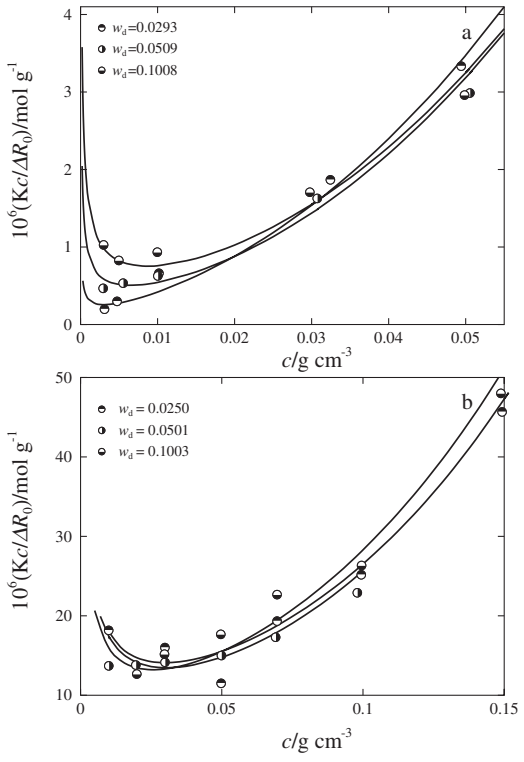

Figure 2. Concentration dependence of $Kc/\Delta R_0$ for the $C_{14}E_6$ micelle solutions at $T = 25.0\,°C$ (a) and for the $C_{10}E_6$ micelle solutions at $T = 40.0\,°C$ (b) containing *n*-dodecane for various w_d indicated. The solid curves indicate the theoretical values.

solutions. Thus we have used the literature values of the density ρ_0 of pure water at corresponding temperatures for ρ, and the values of v of the micelles have been calculated as ρ_0^{-1}.

RESULTS

Cloud Point Curve

Figure 1 illustrates cloud point curves for the ternary system $C_{14}E_6$ + *n*-dodecane + water (a) and $C_{10}E_6$ + *n*-dodecane + water (b), along with the literature results at $w_d = 0$ in (a)[9] and in (b).[11] In panel (a), the triangles at $w_d = 0$ represent the binodal points (see the literature[9] for details). We find that the cloud point curves shift to lower temperatures as w_d increases. All the light scattering experiments have been performed in the L_1 phase below these curves.

SLS Results

In Figure 2a and 2b, $Kc/\Delta R_0$ are double-logarithmically plotted against c for the $C_{14}E_6$ micelle solutions at $T = 25.0\,°C$ and for the $C_{10}E_6$ micelle solutions at $T = 40.0\,°C$ at various w_d, respectively. It is seen that the data points at fixed w_d in these figures follow a curve significantly convex downward and that the data points at different w_d cross with each other. The solid curves indicate the theoretical values calculated as described in detail below.

DISCUSSION

Analysis of SLS Data

As in the previous work mentioned in the Introduction, we have analyzed the present SLS data by employing a light-scattering theory for micellar solutions formulated by Sato[7,8] with a wormlike spherocylinder model for polymer-like micelles in order to determine the M_w values of the micelles at a specified concentration c. The model consists of a wormlike cylinder of contour length $L - d$ with cross-sectional diameter d and two hemispheres of diameter d which cap both ends of the cylinder, and stiffness of the wormlike cylinder is represented by the stiffness parameter λ^{-1}. In the theory, the weight-average molar mass M_w of the micelles and its distribution have been formulated on the basis of multiple equilibria among various micelles of different sizes and monomer, by representing chemical potentials of the micelles as functions of c in a similar fashion to the classical mean-field and recent molecular theoretical approaches.[27–29] In the formulation, the free-energy parameter g_2, which represents the difference in free energy between the surfactant molecules located in the end-capped portion to those in the central cylindrical portion in the micelles, plays a dominant role in the multiple equilibria and then the micellar growth with concentration. The intermicellar thermodynamic interactions have also been taken into account in the chemical potential on the basis of a statistical thermodynamic theory for stiff polymer

solutions with the wormlike spherocylinder model.[8] The interactions also affect the micellar growth to some extent, since they may shift the multiple equilibria among micelles of various sizes through their chemical potentials. The apparent virial coefficient $A(c)$, which includes the second A_2, third A_3, and higher virial coefficient terms, has been formulated to describe thermodynamic properties of micelle solutions up to high concentrations by taking into account the hard-core repulsive interactions dominated by the parameter d together with the attractive interactions dominated by the parameter $\hat{\epsilon}$ (the depth of the attractive potential well) among the micelles.

The expression for $Kc/\Delta R_0$ is written by

$$\frac{Kc}{\Delta R_0} = \frac{1}{M_w(c)} + 2A(c)c \tag{8}$$

where $M_w(c)$ is the weight-average molar mass of the micelles and $A(c)$ is the apparent second virial coefficient. Here, we refer details of the functions $M_w(c)$ and $A(c)$ to the original papers (ref 7 and 8) and our previous papers.[9,11]

As in the case of the previous work,[6] we have treated present micelle solutions as two component systems consisting of micelles and solvent, although they include three components: surfactant $C_{14}E_6$ or $C_{10}E_6$, *n*-dodecane, and water. It has been assumed in the analyses that the composition of ($C_{14}E_6$ or $C_{10}E_6$) + *n*-dodecane in the micelles is given by w_d. The weight average molecular weight of the ($C_{14}E_6$ or $C_{10}E_6$) + *n*-dodecane mixture calculated with a given w_d was used as the surfactant molecular weight M_0 required in the theoretical analysis.

Figure 3a and 3b demonstrate the results of curve-fitting of the theoretical calculations to the experimental values of $Kc/\Delta R_0$ for the micelle solutions of $C_{14}E_6$ at 25.0 °C (a) and of $C_{10}E_6$ at 40.0 °C (b) containing *n*-dodecane with various w_d indicated, respectively. The solid curves which represent the best-fit theoretical curves well coincide with the respective data points at given w_d. The dashed lines represent the values of $1/M_w(c)$ at respective w_d. For the $C_{14}E_6$ micelles at any fixed w_d, they are straight lines with a slope of −0.5, showing that M_w increases with c following a relation $M_w \propto c^{1/2}$ in the range of c examined, as in the case of the previous findings for the micelles formed with single surfactant of various type,[9–14] for those formed with binary C_iE_j mixtures,[15,16] and the micelles containing *n*-dodecanol or *n*-octanol.[2–6] These results are in good correspondence with simple theoretical predictions derived from the thermodynamic treatments of multiple equilibria among micelles of various aggregation numbers.[7,27–29] The increase in $M_w(c)$ with increasing c is also consistent with the findings by Menge *et al.*[30,31] for the $C_{12}E_5$ + *n*-decane micelles.

In contrast to the results, the data points for the $C_{10}E_6$ + *n*-dodecane micelles at fixed w_d follow curves convex upward in qualitative agreement with some of the previous results for the $C_{12}E_5$ and $C_{12}E_7$ micelles containing large amount of *n*-dodecane,[6] implying that these micelles are rather small in length. The solid and dashed curves coincide with each other at small c but the former rapidly increases with increasing c,

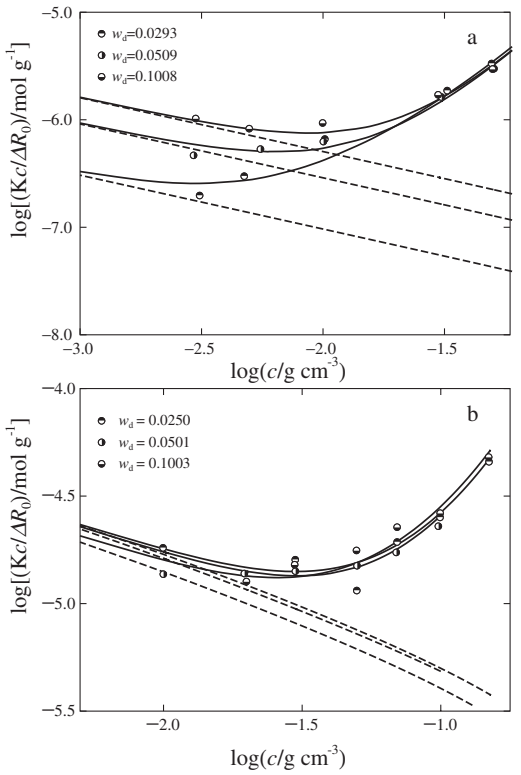

Figure 3. Results of the curve fitting for the double-logarithmic plots of $Kc/\Delta R_0$ against c for the $C_{14}E_6$ + *n*-dodecane + water system at $T = 25.0$ °C (a) and for the $C_{10}E_6$ + *n*-dodecane + water system at $T = 40.0$ °C (b) for various w_d indicated. The solid and dashed curves represent the calculated values of $Kc/\Delta R_0$ and $1/M_w(c)$, respectively.

deviating upward from the latter. The results indicate that contributions of the virial coefficient terms, that is, the second term of the right hand side of eq 8, to $Kc/\Delta R_0$ are negligible at small c but progressively increase with increasing c as expected.

The Micellar Length. Figure 4 illustrates the weight-average length L_w as a function of the surfactant mass concentration c for the $C_{14}E_6$ + *n*-dodecane micelles at $T = 25.0$ °C (a), for the $C_{12}E_6$ + *n*-dodecane micelles at $T = 40.0$ °C (b), and for the $C_{10}E_6$ + *n*-dodecane micelles at 40.0 °C (c), respectively. Here, L_w was calculated by

$$L_w = \frac{4\nu M_w}{\pi N_A d^2} + \frac{d}{3} \tag{9}$$

from the values of M_w and d obtained above from the analyses of the SLS results. For all the micelles with fixed w_d, the length L_w increases with increasing c.

On the contrary, the L_w values of the $C_{14}E_6$ and $C_{12}E_6$ micelles decrease with increasing *n*-dodecane content w_d contrary to the case of the micelles containing *n*-alcohol reported in the previous papers.[2–5] On the other hand, those of the $C_{10}E_6$ micelles increase with increasing w_d, although the degree is rather moderate. The former results may indicate that the addition of *n*-dodecane into the micelles weakens hydrophilic interactions among polyoxyethylene tails of the C_iE_j molecules forming micelles and water too significantly to

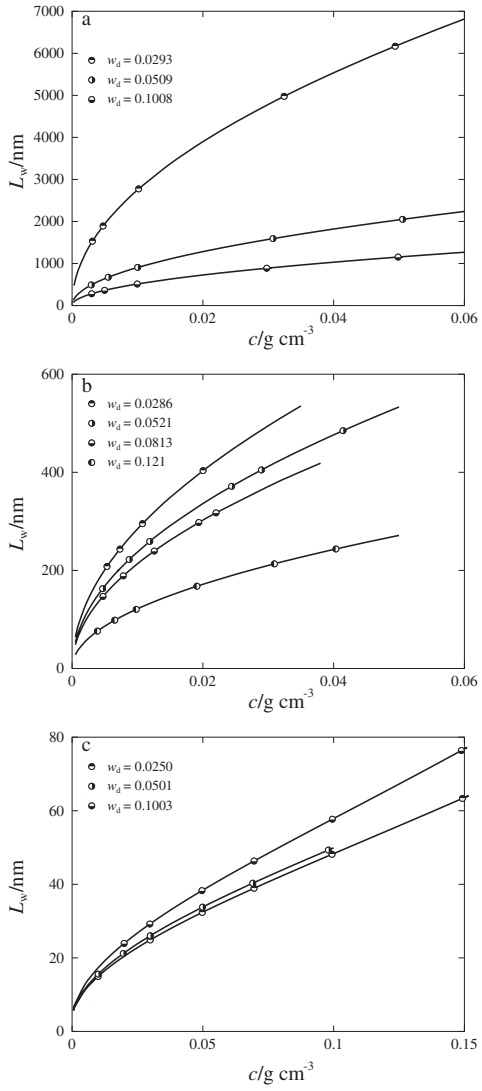

Figure 4. Weight-average micellar length L_w as a function of concentration c for the micelle solutions of $C_{14}E_6$ + *n*-dodecane at 25.0 °C (a), $C_{12}E_6$ + *n*-dodecane at 40.0 °C (b), and $C_{10}E_6$ + *n*-dodecane at 40.0 °C (c) at indicated w_d.

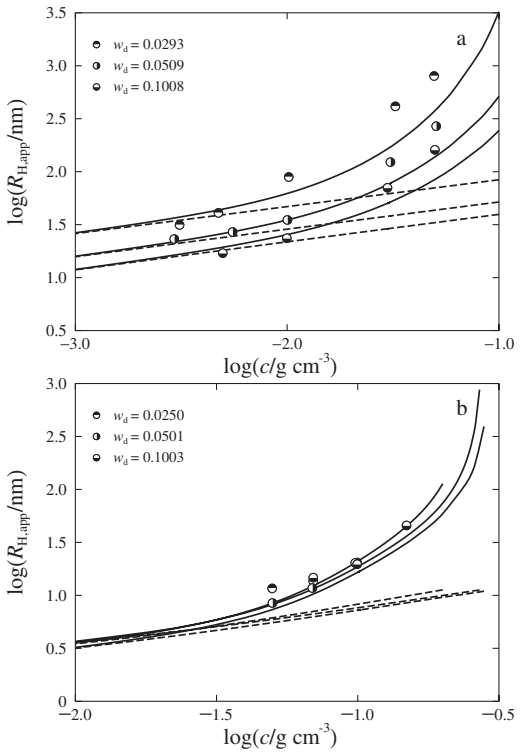

Figure 5. Double-logarithmic plots of the apparent hydrodynamic radius $R_{H,app}$ against c for the $C_{14}E_6$ micelles at $T = 25.0$ °C (a) and for the $C_{10}E_6$ micelles at $T = 40.0$ °C (b) containing *n*-dodecane for various w_d indicated. Solid and dashed curves represent the calculated values with and without the intermicellar hydrodynamic interactions (see the text).

maintain the micellar size as mentioned by Menge *et al.*,[30–32] and leads to collapse of the micelles of smaller size. The results for the micelles including *n*-alcohol may imply that *n*-alcohol play a role of a kind of co-surfactant in the micelles since it has a hydroxyl group which may work as a hydrophilic group.

We see that the L_w value decreases in the order of the $C_{14}E_6$, $C_{12}E_6$, and $C_{10}E_6$ by a factor of 10. Those for the $C_{10}E_6$ + *n*-dodecane micelles are quite small as suggested above from the curve fitting results given in Figure 3b. These results are in part due to the fact that the micellar length L_w is shorter for the surfactant C_iE_j with shorter alkyl chain length i and in part to the fact that L_w become smaller as temperature is decreased apart from the phase boundary.[9–14]

Hydrodynamic Radius of the Micelles

Figure 5a and 5b depict bilogarithmic plots of $R_{H,app}$ determined by eq 7 from the D data against c for the $C_{14}E_6$ + *n*-dodecane micelles at 25.0 °C and for the $C_{10}E_6$ + *n*-dodecane micelles at 40.0 °C of various w_d, respectively. It is seen that at any given w_d, $R_{H,app}$ increases with increasing c. The values of $R_{H,app}$ for the $C_{14}E_6$ + *n*-dodecane micelles at fixed c decrease with increasing w_d, while those for the $C_{10}E_6$ + *n*-dodecane micelles at fixed c scarcely vary with w_d. The increase of $R_{H,app}$ values do not, however, necessarily correspond to that of "isolated" micelles. It reflects both micellar growth in size and enhancement of the effects of the intermicellar hydrodynamic interactions with increasing c. $R_{H,app}$ as a function of c may be represented as

$$R_{H,app}(c) = R_H(c)H(c) \tag{10}$$

where $R_H(c)$ represents the hydrodynamic radius of a "isolated" micelle which grows in size with c and $H(c)$ the hydrodynamic interactions which is enhanced with c. In these two functions, $R_H(c)$ may be calculated by employing the equations formulated for the translational friction coefficient by Norisuye *et al.*[21] with wormlike spherocylinder model near the rod limit and by Yamakawa *et al.*[22,23] with the wormlike cylinder model, as a function of the micellar length L with including d and the stiffness parameter λ^{-1}. Their equation for R_H reads

Polymer Journal

$$R_H = \frac{L}{2f(\lambda L, \lambda d)} \tag{11}$$

The expression for the function f is so lengthy that we refer it to the original papers.[21–23] We are able to calculate $R_H(c)$ required in eq 10, by combining eq 11 with eq 9. Here, L_w by eq 9 is used in place of L in eq 11 and the M_w values as a function of c are obtained from the dashed lines in Figure 3.

The function $H(c)$ in eq 10 may be calculated with the formulation given by Sato *et al.*[17–20] They have recently treated with the concentration dependence of the intermolecular hydrodynamic and direct collision interactions among wormlike polymer chains by using a fuzzy cylinder model. The fuzzy cylinder is defined as a cylinder which encapsulate a wormlike chain or a wormlike spherocylinder in the present case. Its effective length and diameter are evaluated from the wormlike chain parameters L, d, and λ^{-1}. In the formulation, Sato *et al.* have taken into account the hydrodynamic interactions among fuzzy cylinders and also jamming effects of the cylinders on the longitudinal and transverse diffusion coefficients along and perpendicular to the chain end-to-end axis, respectively.

Combining Sato *et al.*'s $H(c)$, eqs 9 and 11 with the experimental results for $M_w(c)$, we have calculated $R_{H,app}(c)$ by eq 10. The solid curves in Figure 5a and 5b are the theoretical values thus calculated. Here, we have used the d values obtained from the analyses of the SLS data and the values of λ^{-1} determined so as to achieve the best fit to the observed results. It is to be noted that the theoretical values of $R_{H,app}$ (and also R_H) for the $C_{10}E_6$ + *n*-dodecane micelles with $w_d = 0.0250$ do not significantly depend on the λ^{-1} value, which is considered to be higher than a few hundreds nm, due to the fact that these micelles are rather small in length. The values of λ^{-1} were not, thus, unequivocally determined for these micelles. The solid (and also the dashed) lines for these micelles represent the theoretical values calculated with $\lambda^{-1} = 200$ nm. The theoretical results for the micelles with a given w_d are in reasonable coincidence with the observed ones, although the data points are somewhat scattered and discrepancy between observed and calculated results are found in some cases. It is found that the theoretical results for $R_{H,app}$ increases more moderately with c than the observed values for the micelle solutions of $C_{14}E_6$ containing *n*-dodecane at large c. The dashed lines represent relationships between R_H and c for the isolated micelles without any intermicellar hydrodynamic interaction, and thus the growth of the micelles with increasing c. We find that the difference between the solid and corresponding dashed lines, *i.e.*, $R_{H,app}$ and R_H, becomes progressively large with c, and that a great portion of $R_{H,app}$ results from the hydrodynamic interactions at large c. On the other hand, the increase of the micellar size with c is rather moderate.

In Figure 6, the same observed and theoretical results for $R_{H,app}$ and R_H as those in Figure 5 are shown as functions of M_w in the bilogarithmic plots. Here, the dashed lines correspond to the theoretical values of R_H calculated by eq 11 combined with eq 9. They asymptotically approach the data points and the solid curves as M_w is decreased, *i.e.*, as c is lowered, indicating that the effects of the intermicellar hydrodynamic interactions on $R_{H,app}$ become negligible in the asymptotic region of low c. The results are in line with our previous findings for R_H of the pure C_iE_j micelles.[9–11] At any given w_d, the difference between the solid and dashed curves, which steeply increase with M_w, is due to the enhancement of the intermicellar hydrodynamic and dynamic interactions with increasing c, *i.e.*, the contribution of $H(c)$ to $R_{H,app}(c)$ in eq 10. For the $C_{14}E_6$ + *n*-dodecane micelles, the data points and the solid line for fixed w_d shift to the smaller M_w and $R_{H,app}$ as w_d is increased contrary to the case of the C_iE_j micelles containing *n*-alcohol, implying that the micelles collapse into smaller size with addition of *n*-dodecane.

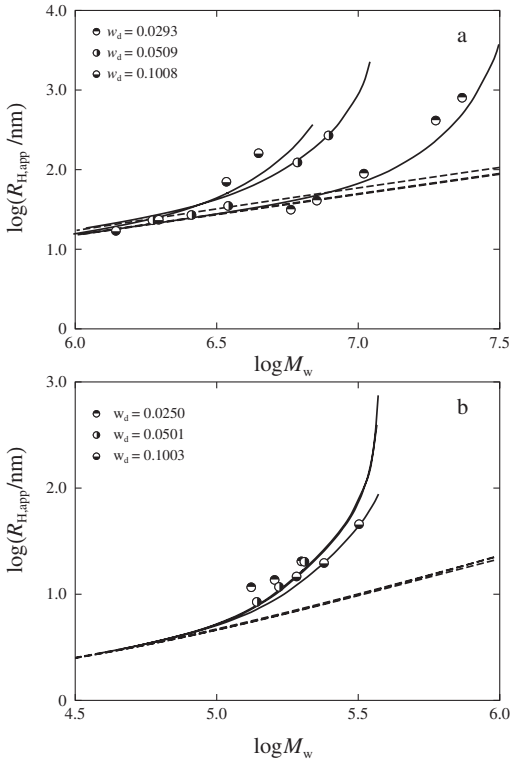

Figure 6. Double-logarithmic plots of the apparent hydrodynamic radius $R_{H,app}$ against M_w for the $C_{14}E_6$ micelles at $T = 25.0\,^\circ$C (a) and for the $C_{10}E_6$ micelles at $T = 40.0\,^\circ$C (a) containing *n*-dodecane for various w_d indicated. Solid and dashed curves represent the calculated values with and without the intermicellar hydrodynamic interactions (see the text).

Variation of Characteristics of the $C_{14}E_6$, $C_{12}E_6$, and $C_{10}E_6$ Micelles with Uptake of *n*-Dodecane

Figure 7 depicts w_d dependence of d for the $C_{14}E_6$ (circles) and $C_{10}E_6$ micelles (squares) containing *n*-dodecane along with the previous results[2] for the $C_{12}E_6$ micelles (triangles) containing *n*-dodecane. The d values of these micelles increase with increasing *n*-dodecane content w_d in the micelles. The present results are similar to the previous findings for the C_iE_j micelles containing *n*-dodecanol or *n*-octanol[3–5] and also those containing *n*-dodecane.[6] They are also in qualitative agreement

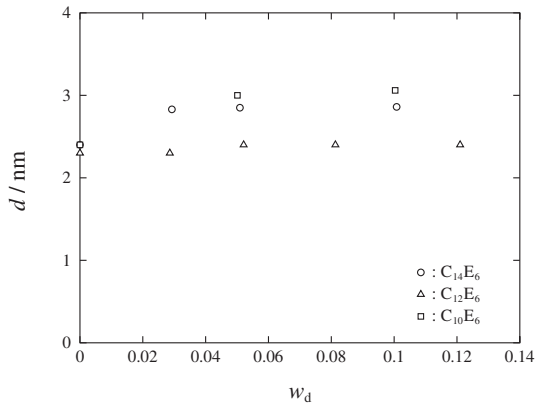

Figure 7. The micellar cross-sectional diameter d as a function of w_d for the $C_{14}E_6$ micelles at 25.0 °C (circles), $C_{12}E_6$ micelles at 40.0 °C (triangles), and $C_{10}E_6$ micelles at 40.0 °C (squares) containing *n*-dodecane.

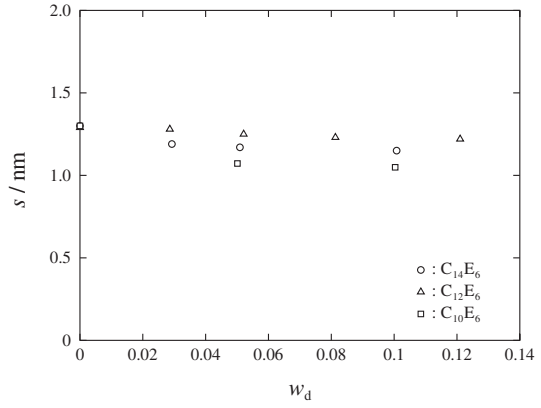

Figure 8. The spacing s of surfactant molecules on the micellar surface as a function of w_d for the $C_{14}E_6$ micelles at 25.0 °C (circles), $C_{12}E_6$ micelles at 40.0 °C (triangles), and $C_{10}E_6$ micelles at 40.0 °C (squares) containing *n*-dodecane.

with SANS results by Menge *et al.*[32] for $C_{12}E_5$ micelles containing *n*-decane. The dependence of the d values on the hydrophobic and hydrophilic chain length is not, however, systematic and thus, we cannot derive definite conclusion about the dependence at present.

The values of the spacing s between the hydrophilic tails of adjacent surfactant molecules on the micellar surface are evaluated from the values of d, L_w, and the aggregation number N_w calculated from M_w. They are plotted against w_d in Figure 8 for the three micelles, *i.e.*, the $C_{14}E_6$ (circles), $C_{12}E_6$ (triangles), and $C_{10}E_6$ micelles (squares) containing *n*-dodecane. The s value is gradually decreased with increasing w_d for the three micelles, implying that the surfactant molecules are more densely assembled as the *n*-dodecane content is increased, in order to keep them inside the micelles. We find that it is substantially independent of the hydrophobic chain length of the surfactant molecules.

Figure 9 illustrates w_d dependence of λ^{-1} evaluated from the analysis of the $R_{H,app}$ *vs* c plots for the $C_{14}E_6$ (circles), $C_{12}E_6$ (triangles), and $C_{10}E_6$ micelles (squares) containing *n*-

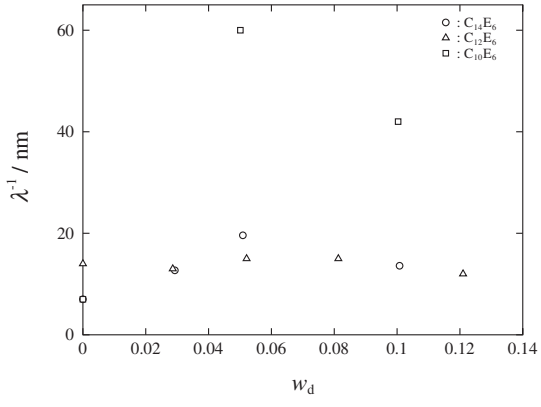

Figure 9. The stiffness parameter λ^{-1} as a function of w_d for the $C_{14}E_6$ micelles at 25.0 °C (circles), $C_{12}E_6$ micelles at 40.0 °C (triangles), and $C_{10}E_6$ micelles at 40.0 °C (squares) containing *n*-dodecane.

dodecane. It is to be noted that the data point for the $C_{10}E_6$ micelle with $w_d = 0.0250$ is missed in this figure since they are too large as mentioned above. It is seen that the λ^{-1} values for the former two micelles do not significantly vary with w_d and that the λ^{-1} values for the $C_{10}E_6$ + *n*-dodecane micelles are larger than those for the other two micelles, although the dependence of the d values on the hydrophilic chain length is not systematic. The fact that the micelles become stiffer with uptake of *n*-dodecane may be correlated with the result that the cross-sectional diameter d of the micelles become larger as *n*-dodecane content is increased in the micelles.

CONCLUSIONS

In the present work, we have examined variation of characteristics of the $C_{14}E_6$ and $C_{10}E_6$ micelles with uptake of *n*-dodecane by static (SLS) and dynamic light scattering (DLS) experiments. As in the previous studies on the C_iE_j micelles containing *n*-alcohol,[2–5] the SLS results $Kc/\Delta R_0$ SLS have been successfully analyzed with the aid of the theory[7,20] for light scattering of micelle solutions formulated with wormlike spherocylinder model, to yield the molar mass $M_w(c)$ as a function of c along with the cross-sectional diameter d of the micelle. The apparent hydrodynamic radius $R_{H,app}(c)$ from DLS as a function of the micellar concentration c has been also successfully analyzed by the fuzzy cylinder theory by Sato *et al.*[17–20] which takes into account the hydrodynamic and direct collision interactions among micelles and allowed us to evaluate the stiffness parameter λ^{-1}.

It has been found that the micellar length L_w increases with increasing c irrespective of the *n*-dodecane content w_d as in the case of the C_iE_j micelles with and without including *n*-alcohol.[2–5,9–14] The d values for all the micelles examined increase with increasing w_d similarly to the micelles containing *n*-dodecanol or *n*-octanol, accompanying the increase of the stiffness parameter λ^{-1}.

On the other hand, the length L_w, molar mass M_w, and hydrodynamic radius R_H of the $C_{14}E_6$ micelles decrease with increasing weight fraction w_d of *n*-dodecane in the micelles

contrary to the micelles including *n*-dodecanol or *n*-octanol, while those of the $C_{10}E_6$ + *n*-dodecane micelles scarcely vary with w_d. The latter values are significantly smaller than those for the former micelles. The former results may result from the fact that the addition of *n*-dodecane into the micelles weakens hydrophilic interactions among polyoxyethylene chains of the surfactant molecules and water, making the micelles unstable and then leading to collapse them into micelles of the smaller size.

Acknowledgment. The authors are grateful to Professor T. Sato of Osaka University for valuable discussions and providing us with the computer program to calculate the apparent hydrodynamic radius.

Received: December 20, 2007
Accepted: January 30, 2008
Published: March 19, 2008

REFERENCES AND NOTES

1. Y. Einaga, Y. Totake, and H. Matsuyama, *Polym. J.*, **36**, 971 (2004).
2. M. Miyake and Y. Einaga, *J. Phys. Chem. B*, **111**, 535 (2007).
3. M. Miyake and Y. Einaga, *Polym. J.*, **39**, 783 (2007).
4. Y. Einaga, M. Ebihara, and R. Uchida, *Polym. J.*, **39**, 792 (2007).
5. M. Miyake, M. Ebihara, and Y. Einaga, *J. Phys. Chem. B*, **111**, 9444 (2007).
6. M. Miyake, A. Asano, and Y. Einaga, *J. Phys. Chem. B*, submitted.
7. T. Sato, *Langmuir*, **20**, 1095 (2004).
8. R. Koyama and T. Sato, *Macromolecules*, **35**, 2235 (2002).
9. S. Yoshimura, S. Shirai, and Y. Einaga, *J. Phys. Chem. B*, **108**, 15477 (2004).
10. N. Hamada and Y. Einaga, *J. Phys. Chem. B*, **109**, 6990 (2005).
11. K. Imanishi and Y. Einaga, *J. Phys. Chem. B*, **109**, 7574 (2005).
12. Y. Einaga, A. Kusumoto, and A. Noda, *Polym. J.*, **37**, 368 (2005).
13. S. Shirai and Y. Einaga, *Polym. J.*, **37**, 913 (2005).
14. Y. Einaga, Y. Inaba, and M. Syakado, *Polym. J.*, **38**, 64 (2006).
15. Y. Einaga, Y. Kito, and M. Watanabe, *Polym. J.*, **38**, 1267 (2006).
16. K. Imanishi and Y. Einaga, *J. Phys. Chem. B*, **111**, 62 (2007).
17. T. Kanematsu, T. Sato, Y. Imai, K. Ute, and T. Kitayama, *Polym. J.*, **37**, 65 (2005).
18. A. Ohshima, A. Yamagata, T. Sato, and A. Teramoto, *Macromolecules*, **32**, 8645 (1999).
19. T. Sato, A. Ohshima, and A. Teramoto, *Macromolecules*, **31**, 3094 (1998).
20. T. Sato and Y. Einaga, *Langmuir*, in press.
21. T. Norisuye, M. Motowoka, and H. Fujita, *Macromolecules*, **12**, 320 (1979).
22. H. Yamakawa and M. Fujii, *Macromolecules*, **6**, 407 (1973).
23. H. Yamakawa and T. Yoshizaki, *Macromolecules*, **12**, 32 (1979).
24. B. Berne and R. Pecora, "Dynamic Light Scattering," J. Wiley, New York, 1976.
25. H. Vink, *J. Chem. Soc., Faraday Trans. I.*, **81**, 1725 (1985).
26. P. Štěpánek, W. Brown, and S. Hvidt, *Macromolecules*, **29**, 8888 (1996).
27. D. Blankschtein, G. M. Thurston, and G. B. Benedek, *J. Chem. Phys.*, **85**, 7268 (1986).
28. M. E. Cates and S. J. Candau, *J. Phys. Condens. Matter*, **2**, 6869 (1990).
29. N. Zoeller, L. Lue, and D. Blankschtein, *Langmuir*, **13**, 5258 (1997).
30. U. Menge, P. Lang, and G. H. Findenegg, *J. Phys. Chem. B*, **103**, 5768 (1999).
31. U. Menge, P. Lang, and G. H. Findenegg, *Colloids Surf., A*, **163**, 81 (2000).
32. U. Menge, P. Lang, G. H. Findenegg, and P. Strunz, *J. Phys. Chem. B*, **107**, 1316 (2003).